

Mapping inflation at Santorini volcano, Greece, using GPS and InSAR

I. Papoutsis,^{1,2} X. Papanikolaou,¹ M. Floyd,³ K. H. Ji,³ C. Kontoes,² D. Paradissis,¹ and V. Zacharis¹

Received 7 October 2012; revised 1 December 2012; accepted 5 December 2012; published 26 January 2013.

[1] Recent studies have indicated that for the first time since 1950, intense geophysical activity is occurring at the Santorini volcano. Here, we present and discuss the surface deformation associated with this activity, spanning from January 2011 to February 2012. Analysis of satellite interferometry data was performed using two well-established techniques, namely, Persistent Scatterer Interferometry (PSI) and Small Baseline Subset (SBAS), producing dense line-of-sight (LOS) ground deformation maps. The displacement field was compared with GPS observations from 10 continuous sites installed on Santorini. Results show a clear and large inflation signal, up to 150mm/yr in the LOS direction, with a radial pattern outward from the center of the caldera. We model the deformation inferred from GPS and InSAR using a Mogi source located north of the Nea Kameni island, at a depth between 3.3 km and 6.3 km and with a volume change rate in the range of 12 million m³ to 24 million m³ per year. The latest InSAR and GPS data suggest that the intense geophysical activity has started to diminish since the end of February 2012. **Citation:** Papoutsis, I., X. Papanikolaou, M. Floyd, K. H. Ji, C. Kontoes, D. Paradissis, and V. Zacharis (2013), Mapping inflation at Santorini volcano, Greece, using GPS and InSAR, *Geophys. Res. Lett.*, 40, 267–272, doi:10.1029/2012GL054137.

1. Introduction

[2] The Santorini volcanic complex is comprised of four islands (Figure 1d): Therassia island and Thera island, well-known touristic destinations, form the caldera rim; Palea Kameni and Nea Kameni have built up in the central caldera. The Santorini caldera has been a source of numerous eruptions and tsunamis in the past with the most recent seismic sequence ending in 1950 [Druitt *et al.*, 1999]. Since then, Santorini volcano was in a “quiet” phase, with insignificant deformation [Stiros *et al.*, 2010; Papageorgiou *et al.*, 2011] and seismic activity limited to a location 10 km northeast of Thera [Dimitriadis *et al.*, 2009]. This phase was interrupted in early 2011, however. Recent GPS and seismic observations show evidence for inflation and increased seismicity within the caldera [Newman *et al.*, 2012]. Further

quantification of the deformation using a multi-interferogram method was presented by Parks *et al.* [2012].

[3] In this study, we present new data (up to September 2012) from a larger, dense network of continuous GPS stations, highlighting the beginning and the end time of the inflation episode in Santorini. Complementary to the stacking technique used by Parks *et al.* [2012], we employ two well-established InSAR methodologies, namely, Small Baseline Subset (SBAS) [Berardino *et al.*, 2002] and Persistent Scatterer Interferometry (PSI) [Ferretti *et al.*, 2001], to produce and analyze the time series of spaceborne SAR data during the period of unrest, resolving and quantifying the deformation history for the total duration of the inflation episode.

2. Input Data and Methodology

2.1. Satellite Interferometry

[4] The only suitable data covering the area of interest for an adequate time span were ENVISAT Advanced Synthetic Aperture Radar (ASAR) data. In October 2010, ENVISAT changed its orbit to a 30-day repeat-pass cycle, and perpendicular baselines over Santorini were optimized. Since mid-April 2012, however, ENVISAT has been unavailable. There is therefore a unique window of opportunity for studying deformation in Santorini under favorable conditions, from March 2011 to March 2012. The SAR data set is comprised of 13 ASAR scenes (Swath 6), descending Track 93, Frame 2882. The lack of ascending pass data was due to ESA's acquisition schedule for the ASAR Global Monitoring mode of operation in the time period of interest. It is noteworthy that the maximum time interval with respect to the 29 September 2011 acquisition (which we use as a reference) is 210 days, while the maximum normal baseline is 411 m, resulting in considerably suppressed geometrical and temporal decorrelation [Zebker and Villasenor, 1992].

[5] The interferometric time series analysis (PSI and SBAS) was performed using the ENVISAT data with the Stanford Method for Persistent Scatterers (StaMPS). This approach was developed to suit volcanic areas and other natural terrains [Hooper *et al.*, 2004]. PSI analysis resulted in the identification of 88,395 PSs, while the SBAS technique identified 278,786 coherent pixels. The two pixel clouds were merged by combining both PSI and SBAS data, leading to 318,250 unique points.

2.2. GPS

[6] In recent years, several institutions have installed continuously operating GPS (cGPS) sites on Santorini, reaching a total of 10 as of September 2012 (Figure 1). However, the majority of sites in this dense network (DSLN, WNRV, SANT, RIBA, MOZI, MKMN) were established after mid-2011. Sites KERA, NOMI, PKMN, and SNTR were established before 2011.

¹School of Rural and Surveying Engineering, National Technical University of Athens, Athens, Greece.

²Institute for Astronomy, Astrophysics, Space Applications and Remote Sensing, National Observatory of Athens, Athens, Greece.

³Department of Earth, Atmospheric and Planetary Sciences, Massachusetts Institute of Technology, Cambridge, Massachusetts, USA.

Corresponding author: I. Papoutsis, School of Rural and Surveying Engineering, National Technical University of Athens, Iroon Polytechniou 9, 15780 Zografou, Athens, Greece. (ipapoutsis@noa.gr)

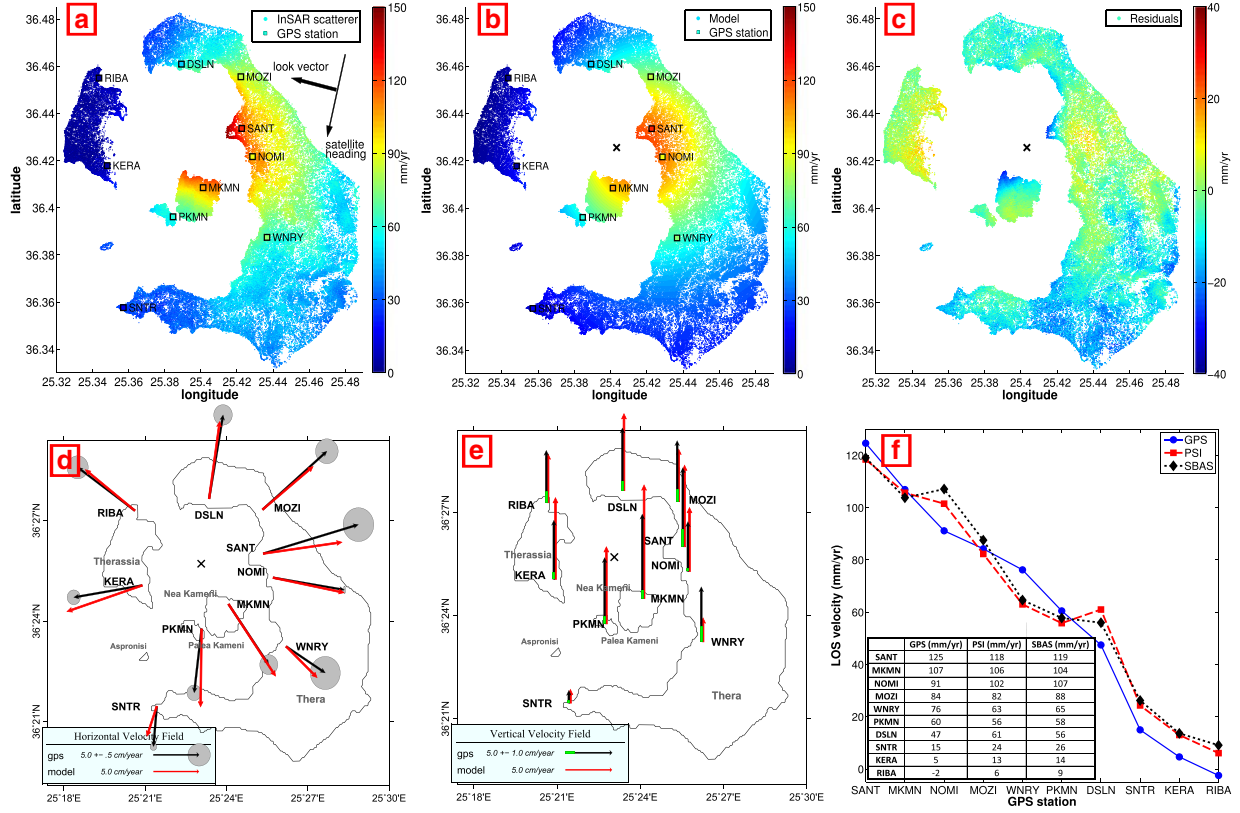


Figure 1. LOS velocities for the (a) merged PSI and SBAS cloud and (b) the best fit parameters of the Mogi model. The MOZI station square corresponds to the reference area, and the colored squares represent the GPS velocities projected to the ENVISAT line-of-sight. (c) Residuals between the model and InSAR measurements. (d and e) Velocities derived from the regression applied on the GPS time series measurements and the corresponding Mogi model, for the horizontal and vertical components, respectively. (f) Comparison between the velocities measured by the different techniques and data sets. The cross symbol represents the Mogi source location derived from InSAR and GPS data.

[7] For the current study, we processed data collected from all 10 receivers, covering the period from January 2010 (where data are available) up to early September 2012. The analysis was carried out using the Bernese GPS Software V5.0 [Dach et al., 2007] with differenced carrier phase observables and IGS final products [Dow et al., 2009] to solve for daily site coordinates and hourly troposphere parameters. The network was tied to an extensive cGPS network covering all of Greece, which was in turn aligned to IGS08, via three no-net-translation conditions imposed on a set of selected fiducial sites [Papanikolaou et al., 2010].

2.3. Interferometry-GPS Compatibility

[8] Satellite interferometry measures deformation \vec{d}_{LOS} along the line-of-sight (LOS) direction between the ASAR sensor and the imaged scene. GPS, on the other hand, measures the 3D displacement vector \vec{d} with components \vec{d}_n , \vec{d}_e , and \vec{d}_u in north, east, and up directions, respectively. Rendering these independent measurements compatible for direct comparison requires re-projecting the GPS vector \vec{d} to the LOS direction [Hanssen, 2001], that is, $\vec{d}_{LOS} = \vec{d} \cdot \vec{l}_{LOS}$, where \vec{l}_{LOS} is the unit vector in the satellite LOS. \vec{l}_{LOS} depends on the incidence angle θ_{inc} ($\sim 39^\circ$ for Swath I6) and the heading angle a_h ($\sim 193^\circ$) of the satellite orbit, which vary across the image swath. For each GPS location, therefore, a unique \vec{l}_{LOS} was defined using the satellite orbital parameters and DEM.

[9] In addition, the deformation derived by interferometric techniques is relative to a reference area in the image. Usually, this is a stable area in the SAR scene that does not exhibit any displacement. In our case, however, this is not feasible due to the large-scale displacement occurring over the entire Santorini complex. Hence, we referenced the LOS velocities derived from PSI and SBAS to an area near the MOZI GPS station (Figure 1). The LOS velocity attributed to this area was the corresponding mean velocity around MOZI, as derived from the GPS time series analysis. This value (84.1 mm/yr LOS) was added to all the remaining PS deformation rates.

[10] The root-mean-square (RMS) differences between the interferometric and GPS velocities are 8.7 and 9.2 mm/yr for PSI and SBAS, respectively. Addressing potential orbital errors by removing a best fit plane from the InSAR results to match all GPS data simultaneously did not lead to noticeable improvement and introduced a bias to the InSAR velocities. Hence, we kept the raw InSAR velocities without subtracting a velocity gradient. The RMS discrepancies in the observed absolute velocity values are about the level expected based on joint data uncertainty [Osmanoğlu et al., 2011] and can be attributed to (i) noise within the SAR data and minor misfits in modeling the interferometric error components, (ii) inherent reduced accuracy in the estimation of the GPS vertical velocity compared to the horizontal components, (iii) limited time span of the InSAR and GPS measurements for robust

velocity estimation, and (iv) existence of unmodeled seasonal (annual and semi-annual) variations, which introduce bias to the velocity estimates.

3. The Unrest Period

3.1. Deformation Field

[11] Inspection of the GPS time series shows a change in velocity for all stations at about the end of February 2012. For example, the east component of SANT (Figure 2d) indicates a change in velocity of approximately 87 mm/yr. This change in motion coincided with a decrease in seismicity within the caldera and the onset of a swarm of seismicity to the SW of Santorini (<http://www.seismicportal.eu>). For that reason, estimation of velocities associated with the inflation was limited to the period from January 2011 up to February 2012. The same approach was adopted for the interferometric time series analysis, by restricting the processed data set not to include the scene acquired in March 2012.

[12] The LOS velocities generated for the merged InSAR data set are shown in Figure 1a, ranging from 150 mm/yr near the source to -10 mm/yr in western Therassia. Selected time series of GPS measurements are depicted in Figure 2. A linear trend was fit to each component of the daily position

time series at each site to estimate the GPS velocities (Figures 1d and 1e). Both independent sets of measurements show the same radial inflation pattern, and Figure 1f depicts the velocities measured by satellite interferometry and GPS in the LOS direction.

3.2. Modeling

[13] We use a Mogi point source [Mogi, 1958] to approximate the inflation episode. The source location is estimated using a linearized least-squares fit of the velocities with respect to horizontal location. This formal inversion confirms the results of a grid search for the best-fitting source location based on the reduced χ^2 of the least-squares fit to the rate of volume change. Both methods show that the InSAR data prefer a source location about 1.5 km to the east of that determined using the GPS data only. The confidence interval contours from the grid search are also elongated and skewed to the north-east, indicating that there is less control on the source location in this direction using the InSAR data. Alternatively, as alluded to by Newman *et al.* [2012], there may be an elongation approximately in the north-south direction of the source itself. The coverage of the InSAR data is also biased to the south and east of the caldera, and we propose that this may be a cause for the location to be resolved closer to the island of Thera. Although

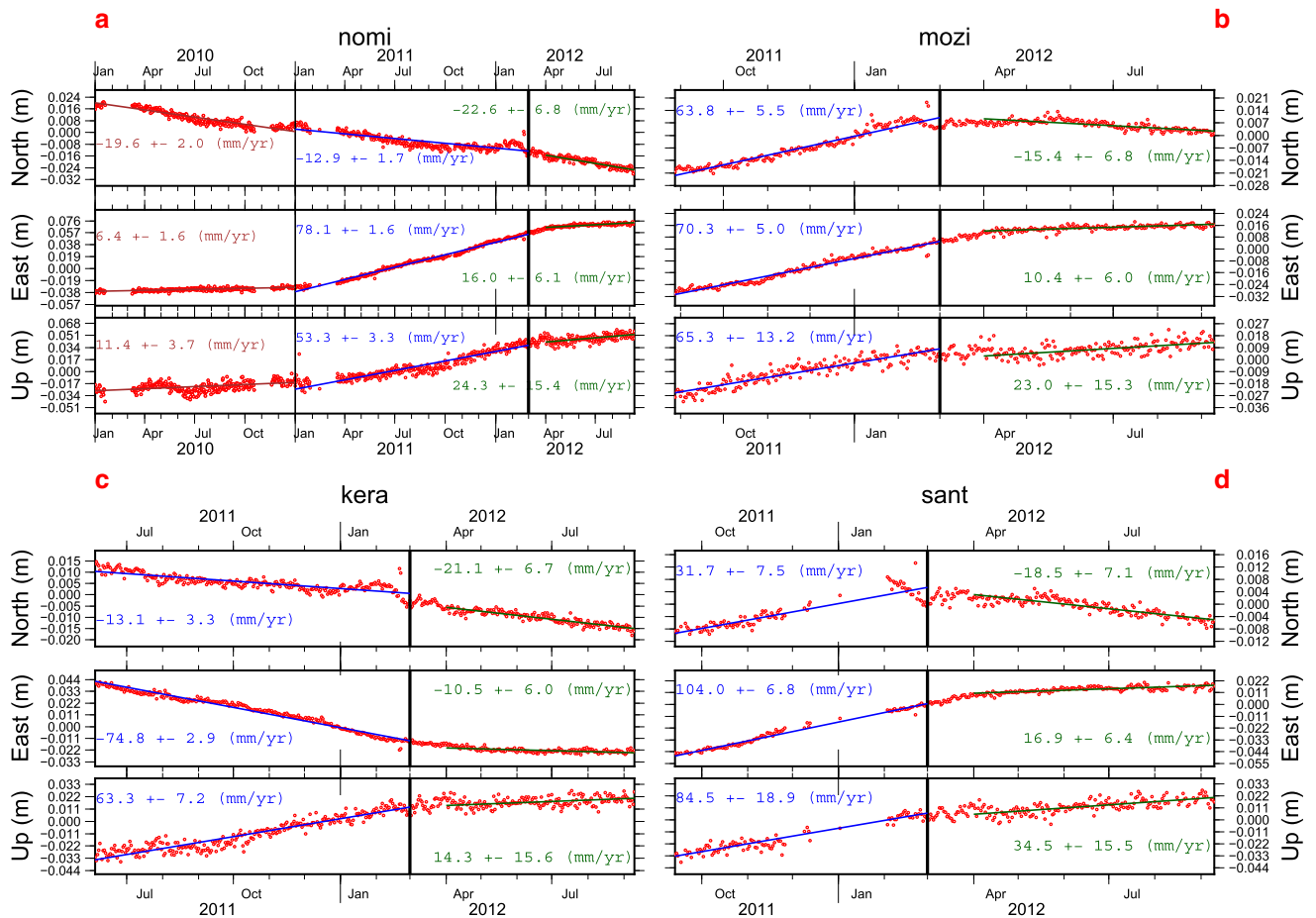


Figure 2. Raw time series of GPS measurements for four selected permanent stations. NOMI station is plotted from January 2010 to highlight the initiation of the strong uplift since January 2011. The thick vertical line corresponds to February 2012, when the phenomenon exhibits a decay in velocity. The velocities derived from the regression analysis are shown for each time span, direction, and GPS station.

the GPS data are sparser in comparison to the InSAR data, the geometry of the GPS network has more balanced azimuthal coverage around the caldera and is therefore probably better for determining the source location.

[14] Due to the strong correlation between source depth and rate of volume change, the probability density functions of these parameters are estimated using a Monte Carlo analysis based on perturbations of the velocities within their uncertainties. The GPS and InSAR data are treated separately with the source location fixed to that estimated using the given data as described above. Table 1 provides the model estimates using GPS only and InSAR only, including their 95% confidence intervals determined by the Monte Carlo analysis.

[15] The reduced χ^2 misfit of the horizontal components of the GPS data (7.6) is larger than that of the vertical component (0.8). This has two possible causes. Either the model is appropriate but the horizontal velocity uncertainties are optimistically small, or the velocity uncertainties are realistic but the model is inappropriate or too simple to explain the horizontal velocities as well as the vertical velocities. *Newman et al.* [2012] test a distributed sill model but consider it unsuitable to explain the observed pattern of deformation. From this, we consider that a penny-shaped crack model will also prove to be unsuitable. We tested the viability of a prolate ellipsoid [*Yang et al.*, 1998] to simulate a vertical crack as an alternative model. This does not produce a significantly better fit to the data and also has large correlations between the aspect ratio of the ellipsoid, rate of volume change and depth.

[16] We propose that the simple Mogi source model is therefore suitable for the modeling of our data (Figures 1b, 1d, and 1e). An arbitrarily more complex source geometry is unlikely to produce a fit that is better than the Mogi source with statistical significance given the number of free parameters. This indicates, however, that our velocity uncertainties, at least in the horizontal component of the GPS data, may be underestimated. This is often the case for GPS velocity uncertainties due to temporally correlated noise in the time series [*Williams*, 2003], which can be difficult to estimate accurately, especially in the presence of transient signals. Santorini is actively deforming so it is difficult to estimate a realistic data noise model for both GPS and InSAR. However, the reduced χ^2 misfits suggest that the uncertainties of the horizontal velocities are underestimated by a factor of 2–3, while those of the vertical components were estimated reasonably. As a result, the uncertainties on the model parameters are also likely to be similarly underestimated.

4. Discussion

[17] The PSI and SBAS techniques presented here implicitly account for and model the error sources in our interferometry data. Using these techniques, we are able to gain accurate line-of-sight velocity estimates and uncertainties in full spatial resolution, which are not possible to assess directly using stacking techniques, as presented by *Parks et al.* [2012]. In

addition, continuous GPS is able to reach levels of uncertainty that allow reasonable analysis more quickly than episodic survey measurements, especially in the case of site accelerations. The expanded cGPS data set presented here compared with that available to *Newman et al.* [2012] provides much improved spatial coverage to constrain better the location of the inflation episode. The longer temporal coverage for our study also allows us to constrain both the onset and end of the 2011 inflation episode. Furthermore, we present a direct comparison of InSAR and GPS data sets for modeling this episode.

[18] Velocity uncertainties are dealt with more explicitly and rigorously in our modeling compared to that by *Newman et al.* [2012] and *Parks et al.* [2012]. Only one or two of *Newman et al.* [2012] vertical velocities are significant outside their associated uncertainties, although *Newman et al.* [2012] do not provide quantitative information on the interval of their velocity confidence ellipses. All GPS uplift rates presented here are significant to beyond a 3-sigma level, which places good constraints on the vertical motion expected from any model.

[19] The evolution of the deformation for Nea Kameni is presented in Figure 3. Reduced deformation is seen in both GPS and InSAR data since February 2012. While up until January 2012, the uplift rate is almost constant, since February 2012 uplift ceased. This pattern is also seen in the deformation behavior observed with the GPS measurements shown in Figure 2. At the NOMI station (Figure 2a), the inflation start date can be identified (January 2011), but from February 2012 onward, a significant change in rate and possibly in the sign of the deformation (Figure 2b and d) is observed. At NOMI, the new velocities estimated for the period from April to September 2012 are comparable to those of the January–December 2010 time span. Finally, the transient subsidence event, seen in Figure 3b, that occurred in February 2012 is also observed in the GPS measurements shown in Figure 2, mostly in the north and up directions.

[20] Differences in the approach between this study, *Newman et al.* [2012] and *Parks et al.* [2012] in terms of presented data type, coverage, and processing technique lead to slight differences in the Mogi source model and associated uncertainties. While all models agree to within their quoted ranges and uncertainties, the correlation between depth and rate of volume change, and the restricted and asymmetric data coverage around the caldera, produces differences in the estimates of these parameters of a factor of two. Locations from GPS and *Parks et al.* [2012] InSAR agree to within ~ 0.5 km, although our InSAR data in this study prefer a location ~ 1.5 km further east. We have previously discussed how this may be due to the asymmetry of the data set.

[21] The source of inflation undoubtedly lies to the north of Nea Kameni. This suggests a complex magma chamber below Santorini which is not necessarily connected directly below the historical center of eruptive activity (the Kameni

Table 1. Mogi Model Parameters for the GPS and InSAR Data

Data set	Longitude	Latitude	Depth/km	$\Delta V/10^6\text{m}^3/\text{yr}$	χ^2/dof^a
3-component GPS	25.3844	36.4286	$3.48^{+0.19}_{-0.17}$	$12.4^{+0.9}_{-0.8}$	9.1
InSAR	25.4033	36.4256	$6.28^{+0.02}_{-0.02}$	$24.2^{+0.1}_{-0.1}$	3.52

^aDegrees of freedom.

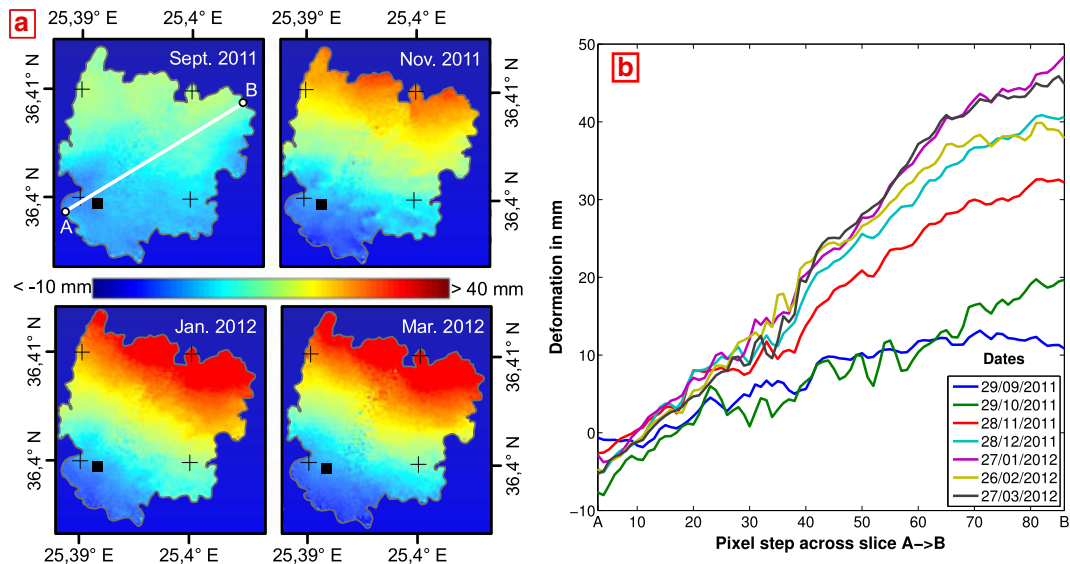


Figure 3. (a) Unwrapped differential interferograms zoomed in on the Nea Kameni region. Master scene is the March 2011 acquisition, and the corresponding slave date is shown at the top-right corner of each interferogram. The black box is the selected reference point. While the magnitude of uplift clearly increases for the first three interferograms, in March 2012 the deformation is similar to the one observed in January 2012. (b) Cumulative deformation in millimeter across slice AB shown in Figure 3a, for selected ENVISAT acquisition dates. Since end of February 2012, an anomaly in the almost constant rate of uplift (up until January 2012) is detected.

islands). It may be that the shallow chamber is fragmented, with lobes or multiple storage areas spread above a deeper reservoir. Alternatively, while the simple Mogi source does fit the available data well within their uncertainties here, the asymmetry of the residuals (Figure 1c) and the tendency for the InSAR data to require the center of inflation to be to the east of that preferred by the GPS data suggest that a more complex model may be more realistic. For example, such a model might consist of magma chamber recharge that is not axi-symmetric and hence may not be accounted for completely by a simple point, spherical, or ellipsoidal source, or evolving location and rate of volume change of the source over time. Such a more complex model is not justified here by the data though.

[22] For the most part, however, this is a relatively simple uplift event suggesting charging of the magma chamber beneath the caldera or permanent redistribution of hydrothermal fluids at depth. There is currently no evidence that this is a transient episode that will reverse; rather, it began and has now returned to previously observed rates of deformation. Although such inflation events are often precursors to eruptive activity, this is not always the case; many examples exist of inflation episodes that did not ultimately result in eruption and were followed by the waning of deformation [Battaglia *et al.*, 2003]. In some cases, these episodes are thought to involve hydrothermal processes rather than emplacement of magma [Gottsmann *et al.*, 2007]. Such episodes require multi-disciplinary studies including gravity, micro-seismicity (tremor activity), and, potentially, surface chemical analyses to verify. The depth of the source determined in this study (3.3–6.3 km), however, would suggest that unless a very deep hydrothermal fluid reservoir exists beneath the caldera, this episode is likely to be one of magmatic inflation of the shallow chamber. The volume associated with this episode of inflation is very small compared to the eruptive

volume of past large eruptions [Parks *et al.*, 2012], although it is comparable to smaller events in recent history (<http://www.volcano.si.edu/index.cfm>).

5. Conclusion

[23] Extensive monitoring of the Santorini volcano with remote sensing techniques and extended geodetic measurements has quantified a period of unrest of the volcano which began in January 2011 and is shown here to have diminished around the end of February 2012. Deformation maps with wide coverage and high accuracy were generated, depicting uplift with a radially decaying pattern in amplitude and velocity from the center of deformation. Maximum inflation of 150 mm/yr, an unprecedented magnitude for Santorini since quantitative monitoring of the area began, is observed at Nea Kameni (a resurgent dome within the caldera), and in Imerovigli and Fira in Thera island (northeast of Nea Kameni). Inversion of the InSAR and GPS data using a Mogi model suggests a source depth of 3.3–6.3 km.

[24] Since February 2012, when the rapid episode ceased, the observed displacement has declined significantly, possibly signaling a new phase of relative stability and reducing the probability of an imminent volcanic eruption, following empirical knowledge from calderas that experienced similar inflation episodes in the past [Newhall and Dzurisin, 1988].

[25] **Acknowledgments.** We would like to thank ESA for the provision of ENVISAT/ASAR data in the framework of ESA-Greece AO project 1489OD/11-2003/72, UNAVCO Facility with support from the NSF and NASA under NSF EAR-0735156 for providing GPS data for some of the stations analyzed in this manuscript, Georgia Tech/University of Patras, COMET and NOANET/NKUA collaboration for providing access to their GPS data. MIT participation was supported in part by NSF Grant EAR-0838488 and NASA Grant NNX09AK68G. We also thank Mike Poland, Jo Gottsmann, Geoff Wadge, and an anonymous reviewer for evaluating this paper and assisting in making it more comprehensive.

References

- Battaglia, M., P. Segall, J. Murray, P. Carville, and J. Langbein (2003), The mechanics of unrest at Long Valley caldera, California: 1. Modeling the geometry of the source using GPS, leveling and two-color EDM data, *J. Volcanol. Geotherm. Res.*, *127*, 195–217, doi:10.1016/S0377-0273(03)00170-7.
- Berardino, P., G. Fornaro, R. Lanari, and E. Sansosti (2002), A new algorithm for surface deformation monitoring based on small baseline differential interferograms, *IEEE. T. Geosci. Remote*, *40*(11), 2375–2383, doi:10.1109/TGRS.2002.803792.
- Dach, R., U. Hugentobler, P. Fridez and M. Meindl (2007), Bernese GPS software, Version 5.0, *Astronomical Institute, University of Bern*.
- Dimitriadis, I., E. Karagianni, D. Panagiotopoulos, C. Papazachos, P. Hatzidimitriou, M. Bohnhoff, M. Rische, and T. Meier (2009), Seismicity and active tectonics at Coloumbo Reef (Aegean Sea, Greece): Monitoring an active volcano at Santorini Volcanic Center using a temporary seismic network, *Tectonophysics*, *465*, 136–149, doi:10.1016/j.tecto.2008.11.005.
- Dow, J. M., R. E. Neilan, and C. Rizos (2009), The International GNSS Service in a changing landscape of Global Navigation Satellite Systems, *J. Geod.*, *83*:191198, doi:10.1007/s00190-008-0300-3.
- Druitt, T. H., L. Edwards, R. M. Mellors, D. M. Pyle, R. S. J. Sparks, M. Lanphere, M. Davies, and B. Barriero (1999), Santorini Volcano, *Geol. Soc. London Mem.*, *19*.
- Ferretti, A., C. Prati, and F. Rocca (2001), Permanent scatterers in SAR interferometry, *IEEE. T. Geosci. Remote*, *39*(1), 8–20, doi:10.1109/IGARSS.1999.772008.
- Gottsmann, J., R. Carniel, N. Coppo, L. Wooller, S. Hautmann, and H. Rymer (2007), Oscillations in hydrothermal systems as a source of periodic unrest at caldera volcanoes: Multiparameter insights from Nisyros, Greece, *Geophys. Res. Lett.*, *34*, L07907, doi:10.1029/2007GL029594.
- Hanssen, R. F. (2001), *Radar Interferometry: Data Interpretation and Error Analysis*, Dordrecht: Kluwer Academic Publishers, 162–163.
- Hooper, A., H. Zebker, P. Segall, and B. Kampes (2004), A new method for measuring deformation on volcanoes and other natural terrains using InSAR persistent scatterers, *Geophys. Res. Lett.*, *31*, L23611, doi:10.1029/2004GL021737.
- Mogi, K. (1958), Relation between the eruptions of various volcanoes and the deformations of the ground surfaces around them, *Bull. Earthq. Res. Inst.*, *36*, 99–134.
- Newhall, C. G., and D. Dzurisin (1988), Historical unrest at large calderas of the world, *U.S. Geol. Survey Bull.* *1855*.
- Newman, A. V., et al. (2012), Recent geodetic unrest at Santorini Caldera, Greece, *Geophys. Res. Lett.*, *39*, L06309, doi:10.1029/2012GL051286.
- Osmanoğlu, B., T. H. Dixon, S. Wdowinski, E. Cabral-Cano, and Y. Jiang (2011), Mexico City subsidence observed with persistent scatterer InSAR, *Int. J. Appl. Earth Observ. Geoinf.*, *13*(1), 1–12, doi:10.1016/j.jag.2010.05.009.
- Parks, M. M., J. Biggs, P. England, T. A. Mather, P. Nomikou, K. Palamartchouk, X. Papanikolaou, D. Paradissis, B. Parsons, D. M. Pyle, C. Raptakis, and V. Zacharis (2012), Evolution of Santorini Volcano dominated by episodic and rapid fluxes of melt from depth, *Nature Geosci.*, doi:10.1038/ngeo1562.
- Papageorgiou, E., M. Fomelis, and I. Parcharidis (2011), SAR interferometric analysis of ground deformation at Santorini volcano (Greece), paper presented at the Fringe 2011 workshop, ESA, Frascati, Italy.
- Papanikolaou, X., A. Marinou, C. Mitsakaki, K. Papazissi, D. Paradissis, V. Zacharis, and D. Anastasiou (2010), An automated processing scheme designed for all available permanent GPS station in Greece, Poster Presented at the 15th General Assembly of the Wegener Project, Istanbul, Turkey.
- Stiros, S. C., P. Psimoulis, G. Vougioukalakis, and M. Fytikas (2010), Geodetic evidence and modeling of a slow, small-scale inflation episode in the Thera (Santorini) volcano caldera, Aegean Sea, *Tectonophysics*, *494*, 180–190, doi:10.1016/j.tecto.2010.09.015.
- Williams, S. D. P. (2003), The effect of coloured noise on the uncertainties of rates estimated from geodetic time series, *J. Geod.*, *76*, 483–494, doi:10.1007/s00190-002-0283-4.
- Yang, X.-M., P. M. Davis, and J. H. Dieterich (1998), Deformation from inflation of a dipping finite prolate spheroid in an elastic half-space as a model for volcanic stressing, *J. Geophys. Res.*, *93*(B5), 4249–4257, doi:10.1029/JB093iB05p04249.
- Zebker, H.A., and J. Villasenor (1992), Decorrelation in interferometric radar echoes, *IEEE. T. Geosci. Remote*, *30*(5), 950–959, doi:10.1109/36.175330.